P H Y S I C A L   R E V I E W   L E T T E R S

Surface-Induced First-Order Transition in Athermal Polymer-Nanoparticle Blends

E. S. McGarrity,[1] A. L. Frischknecht,[2] L. J. D. Frink,[2] and M. E. Mackay[1]

[1]*Department of Chemical Engineering & Materials Science, Michigan State University, East Lansing, Michigan, 48824-1226, USA*
[2]*Sandia National Laboratories, Albuquerque, New Mexico 87185, USA*

We investigate the phase behavior of athermal polymer-nanoparticle blends near a substrate. We apply a recent fluids density functional theory of Tripathi and Chapman to a simple model of the blend as a mixture of hard spheres and freely jointed hard chains, near a hard wall. We find that there is a first-order phase transition in which the nanoparticles expel the polymer from the surface to form a monolayer. The nanoparticle transition density depends on the length of the polymer and the overall bulk density of the system. The effect is due both to packing entropy effects related to size asymmetry between the components and to the polymer configurational entropy. The simplicity of the system allows us to understand the so-called "entropic-push" observed in experiments.

Mixtures of polymers and colloidal-size particles have been shown to exhibit rich phase behavior, in both bulk and near surfaces [1]. The corresponding behavior of blends of nanosize particles and polymers is still being explored and is not well understood. The small size of the nanoparticles leads to both new phenomena [2–4] and potential new applications. Nanoparticles have been shown to migrate to interfaces such as cracks or substrates in experiments, and thus may allow for self-healing surfaces [5]. The self-assembly of nanoparticles in, for example, diblock co-polymers has been studied with the goal of producing composites with useful mechanical, magnetic, and optical properties [6,7].

However, a detailed understanding of the mechanisms by which nanoparticles interact with a polymer matrix near a substrate is lacking. In general, such systems involve a complex admixture of entropic, enthalpic, and chemical interactions between the different components that is difficult to ferret out by experiment. Insight into the physics of polymer nanocomposites can be gained by computational studies of simplified models in order to isolate the individual interactions.

Additionally, interesting phenomena occur even in relatively simple polymer nanocomposites. Recent neutron reflectivity experiments [8,9] have found that in ultrathin films of polymer-nanoparticle mixtures, the nanoparticles often form a monolayer on the substrate. Remarkably, this occurs for the case of polystyrene blended with polystyrene nanoparticles [8], in a regime where the nanoparticles are miscible in the polymer in the bulk [4]. Since the polymer and nanoparticles are chemically compatible, the forces driving the nanoparticles to the substrate are thought to be entropic in origin [9,10]. The presence of about a mono-layer of nanoparticles at the substrate has the additional surprising property of preventing the dewetting of the films.

In this Letter we provide theoretical evidence in support of the hypothesis that purely entropic driving forces can result in nanoparticles segregating to the substrate when blended with a polymer melt. We explore the behavior of the simplest relevant system: a mixture of hard nanoparticles in a hard-chain polymer melt, near a hard surface. An understanding of this system is a prerequisite for understanding more complex situations in polymer nanocomposite films (such as the effect of attractive interactions) since the entropic effects will always be present. As we will show, we find a previously unknown surface phase transition in which the nanoparticles do indeed spontaneously form a monolayer on the substrate.

We employ a computationally efficient, classical density functional theory (DFT) to explore the phase behavior of our model system. DFTs can capture the microscopic structure and thermodynamic behaviors of complex fluids [11,12]. They are based on minimization of a grand potential free energy functional. Since the minimization results in the grand potential free energy of the system, DFTs are well suited to the study of phase behavior. Previous theoretical studies of polymer-nanoparticle mixtures have mostly focused on block copolymers and used various techniques. Recently Sides *et al.* used a hybrid particle-field theory [13] in which the nanoparticles are treated as an external field and the polymer is described with self-consistent field theory (SCFT). Earlier work used a combined SCFT-DFT method [14], with the polymers described by SCFT and the nanoparticles by a DFT. Other works that treated blends with DFT include an examination of the wetting behavior of mixtures of colloids and polymers near the bulk coexistence [15], and an investigation of nanoparticles in diblock copolymer thin films [16]. Here we also treat both the nanoparticles and the polymer within the same, consistent theoretical framework. Our work is the first to examine particles in homopolymer melts near a substrate with DFT.

We use a density functional that is based on the fundamental measure theory of hard sphere liquids, pioneered by Rosenfeld [17]. Both the nanoparticles and the polymer segments are treated as hard spheres. Bonding constraints between the polymer segments are enforced using the

238302-1

Wertheim-Tripathi-Chapman (WTC) bonding functional
[18,19], which is based on Wertheim's thermodynamic
perturbation theory [20,21]. The DFT is formulated in an
open (μVT) ensemble. The grand potential for the hard
sphere–polymer blend is

$$\Omega[\rho_\alpha(\mathbf{r})] = F_{id}[\rho_\alpha(\mathbf{r})] + F_{hs}[\rho_\alpha(\mathbf{r})] + F_{ch}[\rho_\alpha(\mathbf{r})]$$
$$+ \sum_\alpha \int d\mathbf{r}\rho_\alpha(\mathbf{r})[V_\alpha(\mathbf{r}) - \mu_\alpha], \qquad (1)$$

where the terms on the right-hand side represent the
Helmholtz free energies for the ideal gas, the hard sphere,
and the chain constraints. The final term is the Legendre
transformation where the μ_α are the site chemical poten-
tials and $V_\alpha(\mathbf{r})$ is an external field. The exact form of the
Rosenfeld hard sphere term, F_{hs}, can be found in [22]. A
more accessible derivation of this functional can be found
in [23]. We implemented a form of the chain free energy
functional F_{ch} (Eq. 22 from [18]) to keep track of, and
solve explicitly for, segment densities by treating each
segment as a separate species. The Rosenfeld functional
that we use is known to give very accurate density profiles
for binary mixtures of hard spheres [24], while the WTC
functional has been shown to accurately capture the phys-
ics of homopolymers and polymer blends near surfaces
[18,19].

   Minimization of $\Omega[\rho_\alpha(\mathbf{r})]$ leads to a set of nonlinear
integral equations for the density distributions, $\rho_\alpha(\mathbf{r})$, of
the constituent species. We solve the DFT equations using
the TRAMONTO fluids DFT code [25–27], with numerical
methods as detailed elsewhere [28]. The polymers consist
of a chain of N freely- jointed tangent spheres with diame-
ter σ_p while the nanoparticles are hard spheres with di-
ameter $\sigma_n = 2\sigma_p$. We keep the total packing fraction fixed
at $\eta = 0.3665$ unless otherwise noted, where $\eta =
\pi/6(\rho_n\sigma_n^3 + \rho_p\sigma_p^3)$, and ρ_α and σ_α are the species bulk
density and diameter, respectively. The density profiles
were assumed to vary in the z direction only. We performed
our calculations in a large ($L = 80\sigma_p$) box with reflective
boundary conditions to guarantee bulk behavior in the
middle of the box. The external field representing the
hard wall is $V_\alpha = \infty$ for $z/\sigma_p < \sigma_\alpha$ and $V_\alpha = 0$ for
$z/\sigma_p > \sigma_\alpha$.

   We calculated the free energy and density profiles of the
polymer-nanoparticle blend as a function of nanoparticle
concentration. We began by converging a solution at a
nanoparticle density of $\rho_n\sigma_p^3 = 0.001$. We then employed
the arc-length continuation algorithms found in the LOCA
software package [29,30] to trace the free energy of the
system as a function of nanoparticle density, at constant
packing fraction η. This allowed us to find regions of
multiple solutions, with radically different morphologies.

   The surface free energy of a blend with $N = 40$ is shown
in Fig. 1, where the surface free energy is defined as
$\Omega_s[\rho_\alpha(\mathbf{r})] = \Omega[\rho_\alpha(\mathbf{r})] - \Omega_{bulk}$, and Ω_{bulk} is the free en-
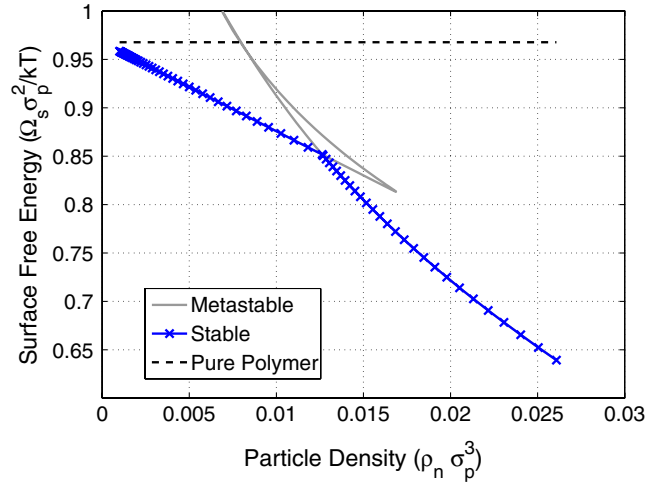ergy of a homogeneous bulk system with the same packing

FIG. 1 (color online).   Surface free energy versus nanoparticle
density for $N = 40$ and $\eta = 0.3665$. The dark curve with the x's
indicates stable configurations. The abrupt change in slope of
this curve at $\rho_n^* = 0.012\,63$ is indicative of a first-order phase
transition. Solutions in the metastable and unstable regions are
shown by the light curve. The dashed line indicates the free
energy of a neat polymer system with $N = 40$ and $\eta = 0.3665$.

fraction and composition. The dark curve with "x"
markers corresponds to the stable solutions of the free
energy minimization for the mixture. There is a distinct
change in slope in the curve at a density of $\rho_n^*\sigma_p^3 =
0.01263$, which indicates a first-order phase transition.
The light part of the curve represents the metastable and
unstable branches of the phase space explored by the
continuation solver. The point at which the curve crosses
itself has two solutions with distinct morphologies. The
dashed line represents the free energy of a neat polymer
system with the same length ($N = 40$) and packing frac-
tion. Note that the addition of nanoparticles reduces the
free energy of the system.

   The two coexisting density profiles found at the phase
transition in Fig. 1 are shown in Fig. 2. A density profile
converged at the coexistence density (ρ_n^*) from a profile at
a slightly lower nanoparticle density is shown in Fig. 2(a).
The density profile is typical for a dense liquid. We see that
both the nanoparticles and polymer have pronounced peaks
near the substrate. The polymer peak is closer to the
substrate because of the smaller size of the polymer seg-
ments. Converging to ρ_n^* from a higher particle density [see
Fig. 2(b)], we find that the polymer has been almost
completely excluded from the vicinity of the substrate,
and there is a large peak in the nanoparticle density adja-
cent to the substrate, indicating a large adsorption of nano-
particles. The height of the first peak in the nanoparticle
density does not change significantly as we add nanopar-
ticles above the transition density, so the structure of the
monolayer remains the same above the transition. The
contact densities are in reasonable agreement with the
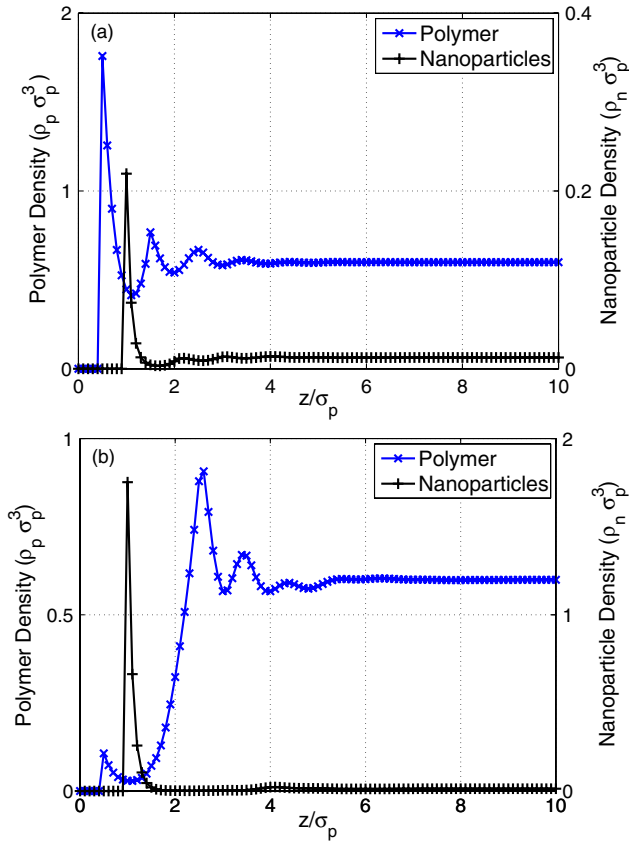pressure sum rule $p/kT = \sum_\alpha \rho_\alpha(z = \sigma_\alpha/2 + \sigma_p/2)$.

FIG. 2 (color online). Density profiles for polymer (x's—left scale) and nanoparticles ($+$'s—right scale), with $N = 40$ with $\eta = 0.3665$ at the phase transition ($\rho_n^* = 0.012\,63$). These profiles were computed by setting the density to ρ_n^* and restarting with an initial guess profile that was converged at a lower (a) and a higher (b) density.

The excess adsorption Γ_α is shown in Fig. 3, where Γ_α is defined as $\Gamma_\alpha = \int_0^\infty dz(\rho_\alpha(z) - \rho_\alpha)$. The vertical lines indicate the sudden jump in adsorption as the nanoparticle density is increased through the phase transition. This jump shows the polymer being expelled from the wall by the nanoparticles with the van der Waals loops being clear indicators of a first-order transition.

Thus we have found a first-order phase transition in which the polymer is pushed away from the substrate and is replaced by the nanoparticles. Integrating under the first peak ($0 \leq z/\sigma_p \leq 2$) of the nanoparticle density profile in Fig. 2(b) gives a density per unit area of $0.2866/\sigma_p^2$, which corresponds to a densely packed monolayer on the surface with an areal coverage of 0.9.

To our knowledge this is the first report of the calculation of an entropically driven surface phase transition in an athermal polymer-nanoparticle blend. We note that unlike other surface phase transitions in similar systems [31–33], our blend does not sit near a corresponding bulk phase transition. Previous studies of binary hard sphere blends have found that there is a fluid-fluid demixing transition only when the size ratio of the particles exceeds 5:1 [22].
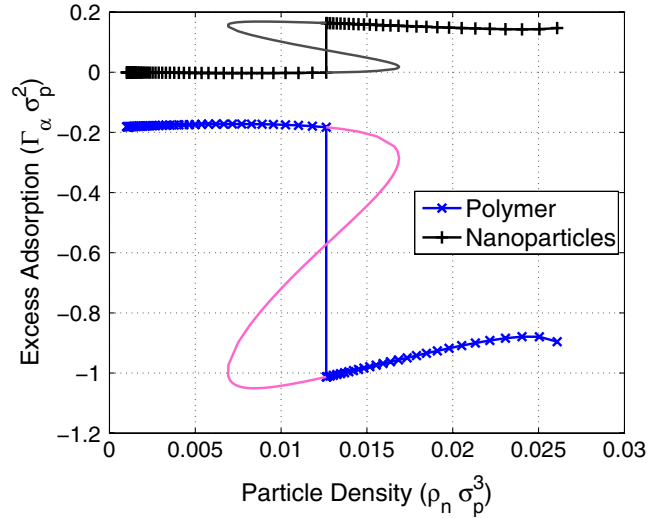

FIG. 3 (color online). Excess adsorption of blend components as a function of nanoparticle density. The x's and $+$'s indicate the polymer and nanoparticles, respectively. The light colored parts of the curves correspond to the metastable and unstable branches.

Paricaud *et al.* [34] showed (for a blend with a similar equation of state to ours) that there is also a first-order fluid-fluid demixing transition in hard polymer–particle mixtures, but only when the particle diameter is larger than about 5 times the monomer diameter. Similar immiscibility for large size asymmetries is predicted by Hooper and Schweizer [35]. Our system should thus be in the regime of bulk miscibility.

In Fig. 4 we show the effects of changing the length of the polymer on the density of the particles ρ_n^* at the transition. Results are shown for two systems, one with a solutionlike packing fraction ($\eta = 0.3665$) and the second with a meltlike packing fraction ($\eta = 0.4152$). In both cases, ρ_n^* decreases with the length of the polymer. For sufficiently short chains ($N \leq 8$ for $\eta = 0.3665$ and $N \leq 5$ for $\eta = 0.4152$), we find no phase transition at all. Also, there is no phase transition for a binary mixture of hard spheres of diameters σ_p and $2\sigma_p$. Thus, the phase transition is a polymeric effect.

The transition must be due to the interplay of chain entropy and packing entropy. One driving force is the well-known depletion potential of a large sphere immersed in a fluid of smaller spheres [36]. This effect leads to enrichment of large spheres near a substrate. Packing entropy should thus help to drive the nanoparticles to the substrate. We note that for particles with the same size as the monomer, $\sigma_n = \sigma_p$, a phase transition is not found, so the particle-monomer size asymmetry is important. A second driving force is the loss of conformational entropy when the polymer is close to the wall. Apparently, the conformational entropy loss is key since the transition only happens for sufficiently long polymers.

To conclude, we have identified a surface-induced first-order phase transition in athermal polymer-nanoparticle
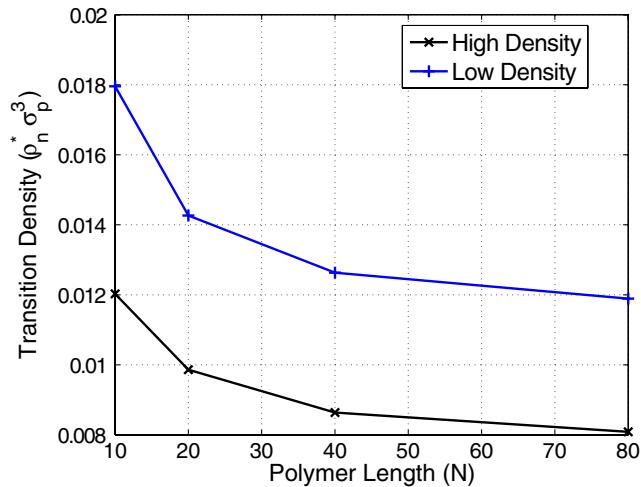
FIG. 4 (color online).   Nanoparticle density at the phase transition as a function of chain length. The $+$'s and x's are for $\eta = 0.3665$ and $\eta = 0.4152$, respectively.

blends. This transition is governed by the polymer chain length and nanoparticle concentration. The existence of a phase transition in such a simple system is noteworthy because the entropic contributions at play here will also be factors in more complex attractive systems. Our work takes a step towards identifying and clarifying the effects of the subtle interplay among entropic contributions originating from size anisotropy and from bonding constraints in polymer-nanoparticle blends.

The existence of this surface phase transition is consistent with the observation of a monolayer of nanoparticles at the substrate in the experiments mentioned previously. We have demonstrated that entropic driving forces alone are sufficient to form a monolayer of nanoparticles at a substrate, adding weight to the "entropic-push" hypothesis used to describe the experimental results [9,10]. In addition, the theory predicts a lowered surface free energy induced by adding nanoparticles to a supported polymer film. The lowered surface free energy may contribute to the observed inhibition of dewetting caused by the addition of nanoparticles [8].

[1] W. C. K. Poon, J. Phys. Condens. Matter **14**, R859 (2002).
[2] A. Tuteja, M. E. Mackay, C. J. Hawker, and B. Van Horn, Macromolecules **38**, 8000 (2005).
[3] J. B. Hooper and K. S. Schweizer, Macromolecules **39**, 5133 (2006).
[4] M. E. Mackay, A. Tuteja, P. M. Duxbury, C. J. Hawker, B. V. Horn, Z. Guan, G. Chen, and R. S. Krishnan, Science **311**, 1740 (2006).
[5] S. Gupta, Q. Zhang, T. Emrick, A. C. Balazs, and T. P. Russell, Nature Mater. **5**, 229 (2006).
[6] M. R. Bockstaller, Y. Lapetnikov, S. Margel, and E. L. Thomas, J. Am. Chem. Soc. **125**, 5276 (2003).
[7] Y. Lin, A. Bôker, J. He, K. Sill, H. Xiang, C. Abetz, X. Li, J. Wang, T. Emrick, and S. Long *et al.*, Nature (London) **434**, 55 (2005).
[8] R. S. Krishnan, M. E. Mackay, C. J. Hawker, and B. V. Horn, Langmuir **21**, 5770 (2005).
[9] R. S. Krishnan, M. E. Mackay, P. M. Duxbury, C. J. Hawker, M. S. Wong, R. Goyette, and P. Thiyagarajan, J. Phys. Condens. Matter **19**, 356003 (2007).
[10] R. S. Krishnan, M. E. Mackay, P. M. Duxbury, A. Pastor, C. J. Hawker, B. V. Horn, S. Asokan, and M. S. Wong, Nano Lett. **7**, 484 (2007).
[11] J. Wu, AIChE J. **52**, 1169 (2006).
[12] J. Wu and Z. Li, Annu. Rev. Phys. Chem. **58**, 85 (2007).
[13] S. W. Sides, B. J. Kim, E. J. Kramer, and G. H. Fredrickson, Phys. Rev. Lett. **96**, 250601 (2006).
[14] R. B. Thompson, V. V. Ginzburg, M. W. Matsen, and A. C. Balazs, Macromolecules **35**, 1060 (2002).
[15] P. Bryk, J. Chem. Phys. **123**, 234907 (2005).
[16] D. Cao and J. Wu, J. Chem. Phys. **126**, 144912 (2007).
[17] Y. Rosenfeld, Phys. Rev. Lett. **63**, 980 (1989).
[18] S. Tripathi and W. G. Chapman, Phys. Rev. Lett. **94**, 087801 (2005).
[19] S. Tripathi and W. G. Chapman, J. Chem. Phys. **122**, 094506 (2005).
[20] M. S. Wertheim, J. Stat. Phys. **35**, 19 (1984).
[21] M. S. Wertheim, J. Stat. Phys. **35**, 35 (1984).
[22] Y. Rosenfeld, M. Schmidt, H. Löwen, and P. Tarazona, Phys. Rev. E **55**, 4245 (1997).
[23] R. Roth, R. Evans, A. Lang, and G. Kahl, J. Phys. Condens. Matter **14**, 12063 (2002).
[24] R. Roth and S. Dietrich, Phys. Rev. E **62**, 6926 (2000).
[25] L. J. D. Frink and A. G. Salinger, J. Comput. Phys. **159**, 407 (2000).
[26] L. J. D. Frink and A. G. Salinger, J. Comput. Phys. **159**, 425 (2000).
[27] http://software.sandia.gov/tramonto (-).
[28] M. Heroux, A. G. Salinger, and L. J. D. Frink, SIAM J. Sci. Comput. (to be published).
[29] *Applications of Bifurcation Theory*, edited by P. H. Rabinowitz (Academic Press, New York, 1977).
[30] A. G. Salinger, E. A. Burroughs, R. P. Pawlowski, E. T. Phipps, and L. A. Romero, Int. J. Bifurcation Chaos Appl. Sci. Eng. **15**, 1015 (2005).
[31] A. Ayadim and S. Amokrane, Phys. Rev. E **74**, 021106 (2006).
[32] P. Bryk and R. Roth, Phys. Rev. E **71**, 011510 (2005).
[33] P. Bryk, J. Chem. Phys. **125**, 204709 (2006).
[34] P. Paricaud, S. Varga, and G. Jackson, J. Chem. Phys. **118**, 8525 (2003).
[35] J. B. Hooper, K. S. Schweizer, T. G. Desai, R. Koshy, and P. Keblinski, J. Chem. Phys. **121**, 6986 (2004).
[36] M. Dijkstra, R. van Roij, and R. Evans, Phys. Rev. Lett. **82**, 117 (1999).